ICHEP94 Ref. gls0231
Submitted to Pa 01
Pl 02

DELPHI 94-95 PHYS 412
1st June, 1994

Measurement of the Forward Backward Asymmetry of charm and bottom Quarks at the Z Pole using $D^{*\pm}$ Mesons

Preliminary

DELPHI Collaboration

Markus Elsing

Abstract

The forward backward asymmetries for the processes $e^+e^- \to c\bar{c}$ and $e^+e^- \to b\bar{b}$ at the Z resonance are measured using identified $D^{*\pm}$ mesons. In 905,000 selected hadronic events, taken in 1991 and 1992 with the DELPHI detector at LEP, 4757 $D^{*+} \to D^{\circ}\pi^+$ decays are reconstructed. The c and b quark asymmetries are determined to be

$$A_{FB}^{c\bar{c}} = 0.081 \pm 0.029\,(\text{stat}) \pm 0.012\,(\text{syst}) \quad \text{and} \quad A_{FB}^{b\bar{b}} = 0.046 \pm 0.059\,(\text{stat}) \pm 0.026\,(\text{syst})\ .$$

Constraining the b asymmetry to the value measured by DELPHI using other independent analyses, the charm asymmetry is measured to be

$$A_{FB}^{c,const} = 0.069 \pm 0.027\,(\text{stat}) \pm 0.011\,(\text{syst})\ .$$

This result corresponds to an effective electroweak mixing angle measured for charm quark events of

$$\sin^2\theta_{eff} = 0.2307 \pm 0.0064\,(\text{stat}) \pm 0.0026\,(\text{syst})\ .$$

1. Introduction

At the Z resonance, the forward backward asymmetries in the differential cross section $d\sigma/d\cos\theta$ for the process $e^+e^- \to f\bar{f}$ result from the interference of vector and axial vector couplings of the initial and final state fermions to the Z boson. In the framework of the Standard Model the integrated Born asymmetry is given by:

$$A_{FB}^{q\bar{q}} \simeq \frac{3}{4} \cdot \frac{2v_e a_e}{v_e^2 + a_e^2} \cdot \frac{2v_q a_q}{v_q^2 + a_q^2} \ .$$

The ratio of the vector coupling v_f and the axial vector coupling a_f depends on the electroweak mixing angle $\sin^2\theta_{eff}$ and a flavour dependent weak vertex correction [1] ($\delta_b = 1$ for b quarks, and 0 otherwise):

$$\frac{v_q}{a_q} = 1 - \frac{2e_q}{I_q^{3L}} \cdot \sin^2\theta_{eff} \cdot (1 + \delta_b \frac{2}{3}\Delta\rho_t) \ , \qquad \text{with} \ \ \Delta\rho_t = 3\frac{G_F m_{top}^2}{8\pi^2\sqrt{2}} \ .$$

In this analysis, the forward backward asymmetries for the processes $e^+e^- \to c\bar{c}$ and $e^+e^- \to b\bar{b}$ at $\sqrt{s} = m_Z$ are measured from the polar angle $\cos\theta$ distribution of charged D^{*+} mesons [1]. The charge of the D^{*+} is directly correlated to the primary quark. A D^{*+} is identified through its decay into $D^\circ\pi^+$, while the D° is reconstructed in the decay modes $K^-\pi^+$, $K^-\pi^+\pi^\circ$ and $K^-\pi^+\pi^-\pi^+$. The energy of the D^{*+} and the decay length of the D° are used to separate $c\bar{c}$ and $b\bar{b}$ events. Particle identification, provided by the DELPHI Ring Imaging Cherenkov Counters (RICH) and the Time Projection Chamber (TPC), is used to reduce the combinatorial background.

After a short description of the D^{*+} reconstruction technique and the particle identification methods, the measurement of the forward backward asymmetries with an unbinned maximum likelihood fit to the D^{*+} spectra, considering the time dependence of the $B_d^\circ - \bar{B}_d^\circ$ mixing effect [4, 5], is described.

2. Detector description and event selection

A detailed description of the DELPHI apparatus has been presented in [6]. For this analysis charged particles measured with the tracking system of DELPHI are used. Here the components relevant to this analysis are briefly described.

The main part of the tracking system is a 2.7 m long Time Projection Chamber, which measures the tracks of charged particles with a resolution of about 250 μm in the $R\phi$-projection (transverse to the beam direction) and 0.9 mm along the z direction (beam direction). For particle identification, the 80% truncated mean of the amplitudes on up to 192 sense wires is used to measure the energy loss per unit of length (dE/dx).

[1] Throughout the paper charge-conjugated states are implicitly included.

The space between the TPC and the beam pipe contains the Inner Detector (ID) and the silicon microstrip Vertex Detector (VD). Each 15° sector of the ID consists of a 24 wire jet chamber surrounded by a 5 layer proportional chamber. The Vertex Detector is built from three concentric shells of 24 silicon microstrip detector modules each 24 cm long. It performs a very good spatial resolution in the $R\Phi$ plane and is therefore the most important detector component of DELPHI for reconstruction of vertices.

In the barrel region (polar angle θ relative to the beam axis between 43° and 137°) the quality of tracking is further improved by the Outer Detector (OD) containing 5 layers of drift tubes. Each layer measures the $R\phi$ coordinate with a resolution of about 110 μm. Three layers also provide an approximate z measurement.

The Barrel RICH, mounted between the TPC and OD, covers a polar angle between 47° and 133°. It identifies the charged particles by measuring the angle of emission of Cherenkov light, and thus the velocity. The mass of the charged particle is then extracted by using the velocity information combined with the momentum measurement provided by the tracking detectors. The DELPHI Barrel RICH uses a liquid (C_6F_{14}) and gas (C_5F_{11}) radiator in order to cover the momentum range 1 to 20 GeV/c.

In the forward and backward regions (θ in the range $11-33°$ or $147-169°$) two additional drift chamber systems improve the tracking. Forward chamber A (FCA) consists of three pairs of wire planes rotated by 120° with respect to each other, in order to resolve ambiguities internally. Forward chamber B (FCB) consists of 12 wire planes twice repeating the orientation of FCA.

2.1 Hadronic event selection

In a first step the primary vertex is fitted iteratively using a beam spot constraint. The beam spot position and its error is determined for each LEP fill of the 1991 data taking period. Due to beam movements in the 1992 data taking period, it is necessary to use different beam spot positions within one LEP fill. For each event the primary vertex is fitted constraining all charged tracks to the beam spot position. In an iterative procedure the tracks with the largest contribution to the overall χ^2 are rejected from the primary vertex fit until the $\chi^2/NDF < 1.5$. The resolution obtained for the fitted primary vertex position perpendicular to the beam axis (xy) is dominated by the VD. It is estimated to be 66(60) μm in $x(y)$ for the 1991 and 50(46) μm in $x(y)$ for the 1992 data. In beam direction (z) the TPC measurement dominates the resolution of about 570 μm and 470 μm, respectively, for the primary vertex.

The complex tracking system of DELPHI requires a track selection depending on the detectors used for the reconstruction. The momentum resolution of tracks at small polar angles, which are reconstructed using only FCA and FCB, is improved by a constraint fit to the primary vertex. A track is discarded if the χ^2 of the constraint fit is larger than 100.

Remaining particles satisfying the following selection criteria enter the analysis:

- track length > 30 cm ,
- $20^\circ \leq \theta_{track} \leq 160^\circ$,
- momentum p between 0.15 and 50.0 GeV/c ,
- relative error on $p < 100\%$,
- impact parameters $\Delta xy \leq 5.0$ cm and $\Delta z \leq 10.0$ cm .

Here the impact parameters Δxy and Δz are calculated relative to the primary vertex. No impact parameter cuts are applied to tracks measured by the FCA and FCB only. Events are accepted if:

- the charged energy $E_{ch} > 12\% \cdot \sqrt{s}$,
- the charged multiplicity $n_{ch} \geq 5$.

These selection cuts ensure a minimal tracking quality and a good agreement of DELPHI data and Monte Carlo simulation. A sample of about 957,000 hadronic events is selected from the data taken by DELPHI in 1991 and 1992, corresponding to a selection efficiency of 96%. Due to the energy dependence of the forward backward asymmetry only events at the Z resonance are used for this measurement. This cut reduces the data sample to about 905,000 events. A sample of 1,118,000 Monte Carlo events including a full detector simulation [7] is used in this analysis.

3. Reconstruction of $D^{*+} \to D^\circ \pi^+$

The D^{*+} is identified through its decay into $D^\circ \pi^+$, while the D° is reconstructed in three different decay channels:

- $K^- \pi^+$
- $K^- \pi^+ \pi^\circ$
- $K^- \pi^+ \pi^- \pi^+$.

For all decay modes the selection of candidates is performed in a similar way. A number of charged tracks corresponding to the multiplicity of the specific D° decay mode are combined, requiring the total charge to be zero. The invariant mass m_{D° of the D° candidate is calculated, assuming one of the particles to be a kaon and the others pions. The π° reconstruction is omitted for the reconstruction of the $K^- \pi^+ \pi^\circ$ decay mode. This leads to a satellite peak at about 1.62 GeV/c^2 below the nominal D° mass. Candidates for the $K^- \pi^+$ and $K^- \pi^+ \pi^\circ$ decay modes are rejected, if their invariant mass is outside of the mass interval 1.1 GeV/$c^2 \leq m_{D^\circ} \leq$ 2.65 GeV/c^2. For the $K^- \pi^+ \pi^- \pi^+$ decay mode the corresponding mass interval is 1.7 GeV/$c^2 \leq m_{D^\circ} \leq$ 2.0 GeV/c^2. A D^{*+} candidate is obtained by assigning a low momentum pion (called slow pion π_{sl} in the following) with opposite charge to the kaon to the reconstructed D°. For all decay modes a secondary vertex fit is performed if the mass

difference Δm between the D^{*+} and the D° is below 200 MeV/c^2 and if the scaled energy $X_E = 2 \cdot E_{D^{*+}}/\sqrt{s}$ of the D^{*+} is greater than 0.175.

The aim of the secondary vertex fit is to obtain the D° flight distance and to improve the track parameters using the additional vertex constraint. Furthermore a reduction of combinatorial background is achieved by rejecting track combinations with large impact parameters with respect to the fitted vertex. As for the track selection, the D° vertex reconstruction method depends on the detectors used in the trackfit. A D° vertex fit using the track information is performed, if at least two tracks are reconstructed in the VD. Otherwise, an additional constraint is used to improve the vertex resolution and thus the D° mass signal, in the sense that the vertex is required to be at the direction of flight of the D° candidate as determined from the momentum vector starting at the primary vertex. The approximation is also sufficient for D° from B decays due to the low impact parameter resolution for tracks without VD. No significant bias on the reconstructed decay length is introduced by this method. Afterwards the slow pion from the D^{*+} decay is constrained to the D° vertex.

The distance between the primary and the D° vertex is calculated in the xy plane and projected on the D° direction of flight to obtain the decay length ΔL. A vertex combination is accepted, if ΔL is within -0.25 cm and 2 cm for the $K^-\pi^+$ and $K^-\pi^+\pi^{\circ}$ decay mode. For the $K^-\pi^+\pi^-\pi^+$ decay mode the interval -0.025 cm $\leq \Delta L \leq 2$ cm is used to reduce the higher combinatorial background. A further reduction of background is achieved by rejecting track combinations with large impact parameters Δxy and Δz with respect to the fitted D° vertex. Therefore the quantity:

$$\chi^2_{\delta} = \begin{pmatrix} \Delta xy \\ \Delta z \end{pmatrix}^T \begin{pmatrix} \sigma^2_{\Delta xy} & cov(\Delta xy, \Delta z) \\ cov(\Delta xy, \Delta z) & \sigma^2_{\Delta z} \end{pmatrix}^{-1} \begin{pmatrix} \Delta xy \\ \Delta z \end{pmatrix}$$

is defined, taking the errors of the impact parameters into account. A vertex combination is rejected if the χ^2_{δ} of a track from the D° candidate is larger than 25 for the two body decay modes and 50 for the $K^-\pi^+\pi^-\pi^+$ decay mode, respectively. For the slow pion, which is constrained to the D° vertex, a maximum χ^2_{δ} of 100 is demanded. Then the vertex information is used to improve the track parameters and thus the invariant mass resolution.

	D° mass interval GeV/c^2	ΔL for D° [cm]	χ^2_{δ} of impact parameter	
			D° tracks	π_{sl} track
$D^{\circ} \to K^-\pi^+$	1.79 - 1.94	-0.25 - 2.0	25	100
$D^{\circ} \to K^-\pi^+\pi^{\circ}$	1.35 - 1.75	-0.25 - 2.0	25	100
$D^{\circ} \to K^-\pi^+\pi^-\pi^+$	1.81 - 1.92	-0.025 - 2.0	50	100

Table 1: Cuts for the D^{*+} selection

Using these improved track parameters, the X_E of the D^{*+} combination is demanded to exceed 0.2. The mass bands to select the different D° decay modes and the cuts on the vertex reconstruction are listed in table 1.

Cuts on the helicity angle distribution (see table 2) are used to achieve a significant reduction of the combinatorial background. The helicity angle $\cos\theta_H$ is defined as the angle of the kaon in the D° rest frame with respect to the D° direction of flight. D° decays are expected to be isotropic in $\cos\theta_H$, whereas the background is extremely peaked at $\cos\theta_H = \pm 1$. For the $K^-\pi^+\pi^-\pi^+$ decay mode similar information is obtained from the sphericity axis of the four particles in the D° system. Due to the energy spectrum of charged tracks in hadronic Z events the combinatorial background is concentrated at small $X_E(D^{*+})$. Therefore X_E dependent cuts are used to account for higher background contributions at small D^{*+} energies:

$D^\circ \to K^-\pi^+$, $D^\circ \to K^-\pi^+\pi^\circ$	$X_E > 0.5 \cdot e^{3\cdot(1\pm\cos\theta_H)} + 0.1$
$D^\circ \to K^-\pi^+\pi^-\pi^+$	$X_E > 0.5 \cdot e^{2\cdot(1\pm\cos\theta_H)} + 0.1$

Table 2: Helicity angle cuts

4. Particle identification

For further reduction of combinatorial background particle identification using barrel RICH information and the dE/dx measurement of the TPC has been applied. Due to the large number of pions in the hadronic final state, the main contribution to the background are $D\circ$ combinations, to which pions is assigned as a kaon candidate. To avoid a reduction of the D^{*+} signal, a pion veto, rather than a kaon identification, has been introduced.

The principle of the pion veto is discussed for the dE/dx-measurement:

At least 30 independent measurements per track are required to obtain the dE/dx information. This condition is fulfilled for 63% of the tracks. A calibration is performed to obtain a standard Gaussian around the correct particle expectation for the measured dE/dx normalized to its error.

The expectation values of dE/dx for kaons and pions are clearly distinguished for momentum p greater than 1.5 GeV/c. Therefore a 1.4σ separation between kaons and pions is obtained by the dE/dx measurement. No dE/dx information is used for particles below 1.5 GeV/c.

In general the light stable particles (π, e, μ) have a higher pion than kaon probability and the heavy stable particles (K, p) vice versa. For this reason a two class separation, which

is necessary for a veto, is obtained by renormalizing the kaon probability density:

$$tag|_{TPC} \;=\; \frac{P_K^{TPC}}{P_K^{TPC} + P_\pi^{TPC}} \cdot 100$$

$P_{K/\pi}^{TPC}$: probability density distribution for kaon/pion expectation .

The π/K separation is shown in figure 1 (a+b) for a pion and an enriched kaon sample from the decay $D^{*+} \to (K^-\pi^+)\pi_s^+$, respectively. The cut on the $tag|_{TPC}$-distribution is X_E dependent to account for the different energy spectra of D^{*+} signal and background. For all analysed decay modes the same cut for the kaon candidates is used as a veto against pions:

$$X_E > e^{\,0.1\cdot(tag|_{TPC}-10)} + 0.1 \; .$$

A similar ansatz for a pion veto is applied using the barrel RICH information. 496000 (235000) events are available with gas (liquid) RICH information in the DELPHI data of 1991 and 1992. For the liquid RICH information a total number of 10 photoelectrons is required. The Monte Carlo simulation was tuned to reproduce the identification efficiency present in the data. The relevant momentum range for kaons from D^{*+} corresponds mainly to the sensitive range of the gas RICH detector. Due to the Cherenkov thresholds for the different particles, a positive identification is not possible over the whole momentum range. Above 3 GeV/c pions radiate light in the gas radiator, while the threshold for kaons is 8 GeV/c. A separation between kaons and pions is possible up to 20 GeV/c, where the expected Cherenkov angles for both hypotheses become saturated. For kaon candidates below 3 GeV/c the liquid RICH information is used.

The different thresholds are taken into account in the calculation of the global probabilities $P_{e,\mu,\pi,K,p}^{RICH}$ from the measured single photon distributions using a maximum likelihood technique [8]. For a pion veto it is sufficient to calculate only the probabilities for pions, kaons and protons, because in the relevant momentum range the Cherenkov angle for light particles is almost maximal and all these particles are treated as pions. Concerning the pion veto the kaon and proton probability can be added. A momentum independent two class separation is obtained by normalizing the probability for kaon and proton to their sum:

$$tag|_{RICH} \;=\; \frac{P_K^{RICH} + P_P^{RICH}}{P_K^{RICH} + P_P^{RICH} + P_\pi^{RICH}} \cdot 100 \; .$$

The pion veto identification for kaons and pions taken from the decay $D^{*+} \to (K^-\pi^+)\pi^+$ is shown in figure 1 (c+d). Due to the good separation quality the cut on the $tag|_{RICH}$ distribution of the kaon candidates is fixed for the whole D^{*+} energy range and for all analysed decay modes:

$$tag|_{RICH} \;\geq\; 25 \; .$$

5. Measurement of $A_{FB}^{c\bar{c}}$ and $A_{FB}^{b\bar{b}}$

For a measurement of $A_{FB}^{c\bar{c}}$ and $A_{FB}^{b\bar{b}}$ from the $\cos\theta$ distribution of D^{*+} it is necessary to separate D^{*+} from c and b events and combinatorial background. Expecting the c and b asymmetry to be of comparable size and to have the same relative sign, the statistical precision of the measurement is limited by the negative correlation between both asymmetries. In this analysis, a good separation, giving a relatively small correlation, is obtained by using the scaled energy distribution X_E of the D^{*+} candidates and the D^0 decay distance to distinguish between the different classes. The hadronization of primary c quarks leads to high energetic D^{*+} mesons, whereas b quarks fragment into B hadrons, which then decay into D mesons with a softer energy spectrum. On the other hand, a larger D^0 decay distance is expected for b events due to the lifetime of B hadrons, which has to be compared to the short living D^0 mesons. This difference was used in [9] to measure the production of D mesons from c and b events separately. The background is concentrated at low X_E and small decay distances. A further constraint on the background in the signal region is obtained from the sidebands in the mass difference distribution. Due to the different acceptance of D^{*+} mesons and background at small and large polar angles, the fit method has to account for the $|\cos\theta|$ dependence of the different classes.

For the asymmetry measurement partially reconstructed D^{*+} mesons and reflections from other decay modes (see figure 2) have to be considered as signal to avoid charge correlations in the background. This leads to a significant increase of the sample, especially for the $K^-\pi^+\pi^0$ decay mode, where about 46% of the signal originates from reflections. The contributions from reflections and true $K^-\pi^+\pi^0$ decays are treated as one class, because of the similar shape of the signals. Since the charge correlation to the primary quark is given by the slow pion from the D^{*+} decay, the rate of partially reconstructed D^{*+} mesons depends on the branching ratio $D^{*+} \to D^0\pi^+$, the D^{*+} production rate and the efficiency for partially reconstructed D^{*+} in the relevant mass difference interval. The contributions of charge correlated background to the D^{*+} signals are taken from the Monte Carlo and give an additional systematic error.

To avoid double counting of events, only the D^{*+} candidate with the D^0 mass closest to the nominal mass is retained. No bias or artificial peak due to this method is introduced in the mass difference distribution, as shown in figure 2. For the $K^-\pi^+\pi^0$ decay mode, the central value of 1.62 GeV/c^2 for the satellite peak is used instead of the D^0 mass. Events entering the $K^-\pi^+$ decay mode are removed from the $K^-\pi^+\pi^-\pi^+$ distribution and events from both decay modes are then removed from the $K^-\pi^+\pi^0$ distribution. The total number of reconstructed D^{*+} decays is given in table 3. The Monte Carlo prediction for the rates of reflections in the D^{*+} signals and the rates of partially reconstructed D^{*+} mesons in the combinatorial background are listed in the third and fourth column, respectively.

decay mode	$D^{*+} \to D^{\circ}\pi^{+}$ events	incl. estimated rate of reflections	rate of $\pi_{sl} + X$ in background
$K^{-}\pi^{+}$	1167 ± 46	4%	11%
$K^{-}\pi^{+}\pi^{-}\pi^{+}$	899 ± 79	8%	18%
$K^{-}\pi^{+}\pi^{\circ}$	2691 ± 143	46%	10%

Table 3: D^{*+} sample used for the measurement

5.1 The unbinned maximum likelihood fit

A precise determination of the asymmetries is achieved by an unbinned maximum likelihood fit (as used in [10]) to the D^{*+} samples using the mass difference, scaled energy, polar angle and D° decay distance distributions. Figures 3-5 compare the measured distributions for the different decay modes with the predictions of the simulation, split into charm, bottom and background events. The Monte Carlo prediction is normalized to the data to reproduce the signal to background ratio. Therefore a factor $R_{S/B}$ is introduced for each decay mode, which compensates for different D^{*+} rates in data and Monte Carlo. After this correction a good agreement is found in all distributions. The shape of the background distribution, as obtained from the sidebands, is well reproduced by the Monte Carlo.

For each decay mode a distance is defined in a four dimensional space:

$$\mathcal{D}_{1,2} = \left\{ \frac{(\Delta m_1 - \Delta m_2)^2}{\mathrm{scale}^2_{\Delta m}} + \frac{(X_{E,1} - X_{E,2})^2}{\mathrm{scale}^2_{X_E}} + \frac{(|\cos\theta_1| - |\cos\theta_2|)^2}{\mathrm{scale}^2_{|\cos\theta|}} + \frac{(\Delta L_{tr,1} - \Delta L_{tr,2})^2}{\mathrm{scale}^2_{\Delta L_{tr}}} \right\}^{\frac{1}{2}} .$$

The transformation $\Delta L_{tr} = \mathrm{sign}\Delta L \ (1 - e^{-2\Delta L})$ of the D° decay distance and a scaling for each distribution (see table 4) are used to obtain an approximately constant density of simulated events around each data point. To calculate the probabilities that a D^{*+} candidate belongs to the different classes, the N_{MC} Monte Carlo generated events with the smallest distance $\mathcal{D}_{1,2}$ to the data event are collected. For this analysis $N_{MC} = 50$ is chosen for the $K^{-}\pi^{+}$ decay mode and $N_{MC} = 100$ for the $K^{-}\pi^{+}\pi^{-}\pi^{+}$ and $K^{-}\pi^{+}\pi^{0}$ decay modes, which is optimized to the available statistics. The probability for each data event to be a charm, bottom or background event is given by:

$$P_k(\Delta m, X_E, |\cos\theta|, \Delta L_{tr}) = \frac{N_k}{N_{MC}} \cdot R_{S/B} \ .$$

Here N_k is the number of Monte Carlo events from class k, while k stands for charm, bottom or background, respectively. The asymmetry for a fixed polar angle then determines the contribution to the log likelihood according to the different classes:

$$F_k(\theta, A_k) = \frac{1}{2}\left(1 + \frac{8}{3} A_k \frac{\cos\theta}{1 + \cos^2\theta}\right) \ ,$$

where A_k is the integrated asymmetry of class k, which in case of the b asymmetry includes a correction for $B-\bar{B}$ oscillation effects (see section 5.2). Then the negative logarithm of the likelihood function to be minimized is obtained combining the information from all decay modes:

$$\mathcal{L} = -ln\left\{\prod_{j=1}^{N_{Data}}\sum_{k=1}^{3} P_{k,j}F_k(\theta_j, A_k)\right\} .$$

decay channel	N_{MC}	scales				$R_{S/B}$
		Δm $[MeV/c^2]$	$\lvert\cos\theta\rvert$	X_E	ΔL_{tr}	
$K^-\pi^+$	50	1.0	0.2	0.1	0.15	88 %
$K^-\pi^+\pi^-\pi^+$	100	1.0	0.2	0.1	0.15	102 %
$K^-\pi^+\pi^\circ$	100	2.0	0.2	0.1	0.15	105 %

Table 4: Scales and normalization factors used in the calculation of the probabilities

5.2 $B-\bar{B}$ oscillation effects

To obtain the b quark asymmetry, the effective D^{*+} asymmetry observed in bottom events has to be corrected for mixing of neutral B mesons:

$$A_{FB}^{b\bar{b},mix} = (1-2\chi)\cdot A_{FB}^{b\bar{b}} .$$

Since the D° decay length is used to separate charm and bottom events, the time dependence of the $B_d^\circ - \bar{B}_d^\circ$ oscillation effect, first observed in [4], needs to be taken into account. Due to the missing momentum reconstruction, the B_d° proper decay time cannot be calculated. Using the average Lorentz boost $\gamma\beta$ of B_d° mesons, the dependence of the $B_d^\circ - \bar{B}_d^\circ$ oscillation can be parameterized as a function of the sum of the B_d° and D° decay lengths ΔL:

$$\chi(\Delta L) = \frac{1}{2}\left\{1-\cos\left(x_d\cdot\frac{\gamma\beta\Delta L}{\tau_{B_d^\circ}}\cdot a_1\right)\cdot(1-a_2\Delta L)\right\} . \qquad (1)$$

The world average values for $x_d = \Delta m_d/\Gamma = 0.69\pm0.07$ [2] and $\tau_{B_d^\circ} = 1.53\pm0.09$ ps [3] are taken for the oscillation frequency and the B_d° lifetime, respectively. The correction factors $a_1 = 0.7$ and $a_2 = 0.14$ are obtained from Monte Carlo simulation, taking also vertex resolution effects into account. A lifetime independent scheme is applied to correct for $B_s^\circ - \bar{B}_s^\circ$ oscillation, using $\chi_s = 0.4-0.5$ as expected by the Standard Model.

The individual contributions to the D^{*+} production from different B decays are obtained from the JETSET 7.3 Monte Carlo model [11]. The production rates of B mesons from a b quark are set to 0.43 for B_d° and B_u^+ and to 0.095 for B_s° respectively. The ratio $\frac{V}{V+P}$ is assumed to be 0.75 for b and c events. The production rate of p-wave mesons is adjusted to

24%, leading to a ratio of D^* to D mesons in agreement with recent measurements [9, 12]. The relative rates of the different $L = 1$ states are determined by their spin weight. As listed in table 5, the main contribution to the D^{*+} production is given by B_d° decays, while the production from B_u^+ and B_s° is suppressed. The inclusive branching ratio $B_{d,u} \to D^{*+} + X$ is in agreement with the recent measurement of $(26.9 \pm 3.5)\%$ [14]. Contributions from decays of B_c^+ mesons, b baryons and fragmentation of b quarks are found to be of minor importance. Another process, leading to an observed asymmetry with negative sign, is the decay $\bar{b} \to W^+ \to c \to D^{*+}$. Its rate is expected to be less than 2%.

$\bar{B}^\circ \to D^{*+} + X$	71%	$(1 - 2\chi_d(\Delta L)) \cdot A_{FB}^{b\bar{b}}$
$B^- \to D^{*+} + X$	21%	$A_{FB}^{b\bar{b}}$
$\bar{B}_s^\circ \to D^{*+} + X$	3%	$(1 - 2\chi_s) \cdot A_{FB}^{b\bar{b}}$
$\bar{b} \to W^+ \to c \to D^{*+}$	2%	$-A_{FB}^{b\bar{b},mix}$
others *	3%	~ 0

* fragmentation, B_c , $b - baryon \to D^{*+} + baryon$ ...

Table 5: Relative contributions to the D^* sample from b events, as obtained from the Monte Carlo

5.3 The fit result

Taking into account the lifetime evolution of the $B_d^\circ - \bar{B}_d^\circ$ oscillation, a three parameter fit of the charm, bottom and background asymmetry to the combined D^{*+} sample yields:

$$A_{FB}^{c\bar{c}} = 0.081 \pm 0.029\,(\text{stat}) \quad \text{and} \quad A_{FB}^{b\bar{b}} = 0.046 \pm 0.059\,(\text{stat})\,,$$

with a correlation coefficient of -38%. The background asymmetry A_{FB}^{back} is found to be $-0.001 \pm 0.009\,(\text{stat})$. Furthermore, no asymmetry is observed in the background of the individual decay modes. The results of the fit to the individual decay modes are listed in table 6.

A two parameter fit of the constrained charm asymmetry $A_{FB}^{c,const}$ and A_{FB}^{back} is performed using $A_{FB}^{b\bar{b}} = 0.102 + 0.059 \cdot A_{FB}^{c,const}$ from the DELPHI measurement [15] using prompt leptons and lifetime tag to reduce the error on the charm asymmetry. From this asymmetry the effective D^* asymmetry is calculated taking the oscillation of neutral B mesons into account. A two parameter fit to the data yields:

$$A_{FB}^{c,const} = 0.069 \pm 0.027\,(\text{stat})$$

	$A_{FB}^{c\bar{c}}$	$A_{FB}^{b\bar{b}}$	A_{FB}^{back}
$K^-\pi^+$	6.3 ± 5.4	9.1 ± 9.6	0.5 ± 4.2
$K^-\pi^+\pi^-\pi^+$	7.8 ± 6.1	7.3 ± 13.0	-0.7 ± 1.9
$K^-\pi^+\pi^\circ$	9.3 ± 4.3	-0.9 ± 9.7	0.2 ± 1.2

Table 6: Fit results of the three parameter fit to the individual decay modes

The program ZFITTER[16] is used to obtain the effective electroweak mixing angle $\sin^2\theta_{eff}$ for charm quark events, using $m_Z = 91.187$ GeV/c^2, $m_{top} = 175$ GeV/c^2 [17], $m_H = 300$ GeV/c^2 and $\alpha_s(m_Z) = 0.123$ [18] as central values to calculate the radiative corrections. For the data sample the average center of mass energy is $\sqrt{s} = 91.270 \pm 0.035$ GeV. The effective electroweak mixing angle, as defined in section 1, is measured as:

$$\sin^2\theta_{eff} = 0.2307 \pm 0.0064\,(\text{stat})\ .$$

6. Systematic errors

Differences between the signal and background efficiency as a function of $\cos\theta$ are considered in the calculation of the probabilities from the Monte Carlo simulation. Since the asymmetry enters in the likelihood as a function of $\cos\theta$, the sensitivity on efficiency variations is small.

For all decay modes the relative normalization $R_{S/B}$ is obtained from a fit of the Monte Carlo D^{*+} signal and background to the data. A $\pm 15\%$ variation is included in the systematic error, not only to account for the error of the fitted $R_{S/B}$, but also for uncertainties in the agreement of the shape of the signals in data and Monte Carlo.

The Monte Carlo simulation is tuned to reproduce the production rates and the average energy of D^{*+} mesons in charm and bottom events as measured by the LEP experiments [9, 12, 13]. A $\pm 15\%$ variation of the ratio of charm to bottom events is considered in the systematic error. The error due to the uncertainty of the average D^{*+} energy is considered by varying the average energy fraction carried by b hadrons between 0.67 and 0.72 and the average D^{*+} energy in c events between 0.48 and 0.52.

In the Monte Carlo simulation a B lifetime $\tau_B = 1.6$ ps is used, which is in good agreement with the world average [3]. A variation between 1.35 and 1.85 ps is considered in the determination of the systematic error.

The uncertainty on τ_B also affects the B_d° oscillation correction for the bottom asymmetry. The measured oscillation frequency $x_d = \Delta m_d/\Gamma = 0.69 \pm 0.07$ [2] is used for the calculation. The errors assigned to the correction factors a_1 and a_2 in equation 1 include resolution effects on the D° vertex.

The influence of the mixing effect on the observed b asymmetry depends on the relative contributions to the b sample. The systematic error is determined by changing the composition of the b sample according to the Monte Carlo study mentioned above. The influence

of the uncertainty on χ_s is found to be negligible.

The systematic error due to the charge correlated background from partially reconstructed D^{*+} decays is estimated by a 30% variation of the contribution predicted from the Monte Carlo. This includes uncertainties on the efficiency to reconstruct such $\pi_{sl} + X$ combinations as well as on the total rate of $D^{*+} \to D^{\circ}\pi^{+}$ decays in hadronic Z events. The systematic error accounts also for the uncertainty of the B°_{d} oscillation correction, because the reconstructed vertex for $\pi_{sl} + X$ combinations is shifted to smaller decay distances.

The systematic error due to the fitting method and the limited statistics of the Monte Carlo reference sample is derived from simulation studies. The stability of the fit is tested by a uncorrelated 30% variation of the scales entering the distance function $\mathcal{D}_{1,2}$ and the number of Monte Carlo events N_{MC} used to determine the probabilities in the likelihood function.

systematic error source	$A_{FB}^{c\bar{c}}$	$A_{FB}^{b\bar{b}}$	$A_{FB}^{c,const}$	$sin^2\theta_{eff}$
normalization $\frac{signal}{background}$	∓ 0.003	∓ 0.002	∓ 0.003	± 0.0008
$(\gamma_c \cdot P_{c\to D^*})/(\gamma_b \cdot P_{b\to D^*})$	∓ 0.002	± 0.001	∓ 0.001	± 0.0002
$\langle x_c \rangle$	± 0.001	± 0.002	± 0.001	∓ 0.0003
$\langle x_b \rangle$	± 0.001	∓ 0.001	∓ 0.001	± 0.0001
τ_b	± 0.002	∓ 0.004	∓ 0.001	± 0.0002
B°_{d} oscillation	∓ 0.003	± 0.012	± 0.002	∓ 0.0005
contributions to b sample	∓ 0.002	± 0.005	± 0.002	∓ 0.0004
rate of $\pi_{sl} + X$	∓ 0.006	± 0.009	∓ 0.005	± 0.0011
fit method	± 0.006	± 0.015	± 0.005	∓ 0.0012
MC statistics	± 0.005	∓ 0.009	± 0.005	∓ 0.0010
detector effects	± 0.004	± 0.002	± 0.004	∓ 0.0010
D^* instead of quark direction	± 0.001	± 0.001	± 0.001	∓ 0.0002
$\Delta A_{FB}^{b\bar{b}}$ for constraint fit	–	–	∓ 0.003	± 0.0007
uncertainties of $m_{top}, m_H, m_Z, \alpha_s, \sqrt{s}$	–	–	–	± 0.0004
total	0.012	0.024	0.011	0.0026

Table 7: Contributions to the systematic errors on the measured asymmetries and $sin^2\theta_{eff}$. The estimated correlation between the systematic errors of $A_{FB}^{c\bar{c}}$ and $A_{FB}^{b\bar{b}}$ in the combined fit is -22%

A shift in the central value as well as in the width of the reconstructed invariant mass distribution for D° mesons relative to $\bar{D}^{\circ}$ mesons, which is furthermore different in both detector hemispheres, can also affect the asymmetry measurement. An upper limit for the systematic error on the charm asymmetry is ± 0.004 and ± 0.002 for the bottom asymmetry, taking the energy dependence of the width of the reconstructed D° mass distribution into

account.

The error of the asymmetry due to the determination of the primary quark direction by the D^{*+} direction is derived from the predictions of different Monte Carlo models.

The error of the constrained fit of the charm asymmetry, using the DELPHI b asymmetry measurement from prompt leptons and lifetime tag, is obtained from the errors quoted in [15]. The additional error of $sin^2\theta_{eff}$ due to the uncertainties of m_{top}, m_H, m_Z, α_s and $\sqrt{s}$ is obtained by a variation of m_Z and α_s within their errors, while $\sqrt{s}$ is varied by ± 35 MeV around the average value. The influence of the top and Higgs mass is found to be of minor importance.

The contributions to the systematic errors for the combined fit of the charm and bottom asymmetries and for the constrained fit are listed in table 7. The relative sign of the systematic error indicates the direction in which the results change for a particular error source. The estimated correlation between the systematic errors of $A_{FB}^{c\bar{c}}$ and $A_{FB}^{b\bar{b}}$ in the combined fit is -36%.

7. Conclusion

The forward backward asymmetries for charm and bottom quarks at the Z pole are measured simultaneously from the mass difference, scaled energy, polar angle and D° decay distance distributions of 4757 D^{*+} mesons using a unbinned maximum likelihood fit. Taking the lifetime evolution of the $B_d^\circ - \bar{B}_d^\circ$ oscillation into account, the fit yields:

$$A_{FB}^{c\bar{c}} = 0.081 \pm 0.029\,(\text{stat}) \pm 0.012\,(\text{syst}) \quad \text{and} \quad A_{FB}^{b\bar{b}} = 0.046 \pm 0.059\,(\text{stat}) \pm 0.026\,(\text{syst})\ .$$

The total correlation between $A_{FB}^{c\bar{c}}$ and $A_{FB}^{b\bar{b}}$ is -36%. Constraining the b asymmetry to the value measured by DELPHI using prompt leptons and lifetime tag [15], the charm asymmetry is determined to be:

$$A_{FB}^{c,const} = 0.069 \pm 0.027\,(\text{stat}) \pm 0.011\,(\text{syst})\ .$$

This result corresponds to an effective mixing angle measured for charm quarks events of:

$$\sin^2\theta_{eff} = 0.2307 \pm 0.0064\,(\text{stat}) \pm 0.0026\,(\text{syst})\ .$$

Good agreement with recent results from other experiments [12, 13] is found.

Figures

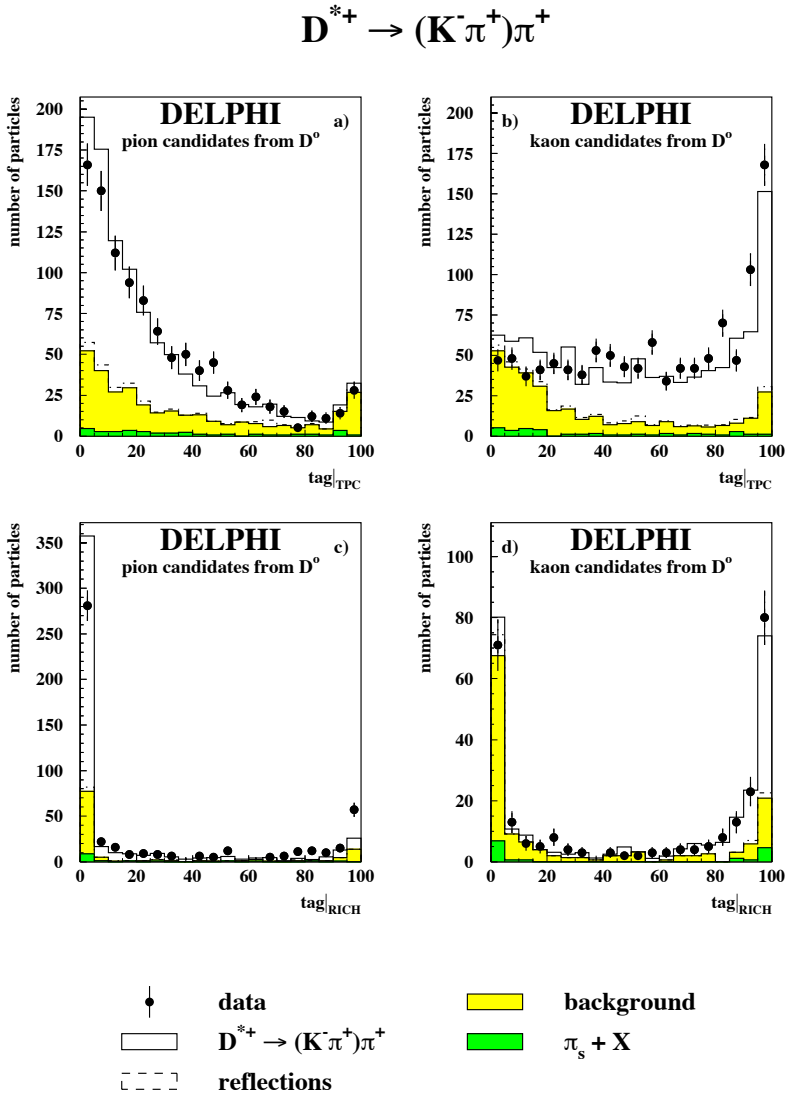

Figure 1: Separation between kaons and pions using dE/dx in the TPC for a pion (a) and an enriched kaon (b) sample obtained in $D^{*+} \rightarrow (K^-\pi^+)\pi^+$ decays. The pion and kaon/proton separation obtained by the RICH information is shown in (c) and (d). See section 4 for the definition of $tag|_{TPC}$ and $tag|_{RICH}$.

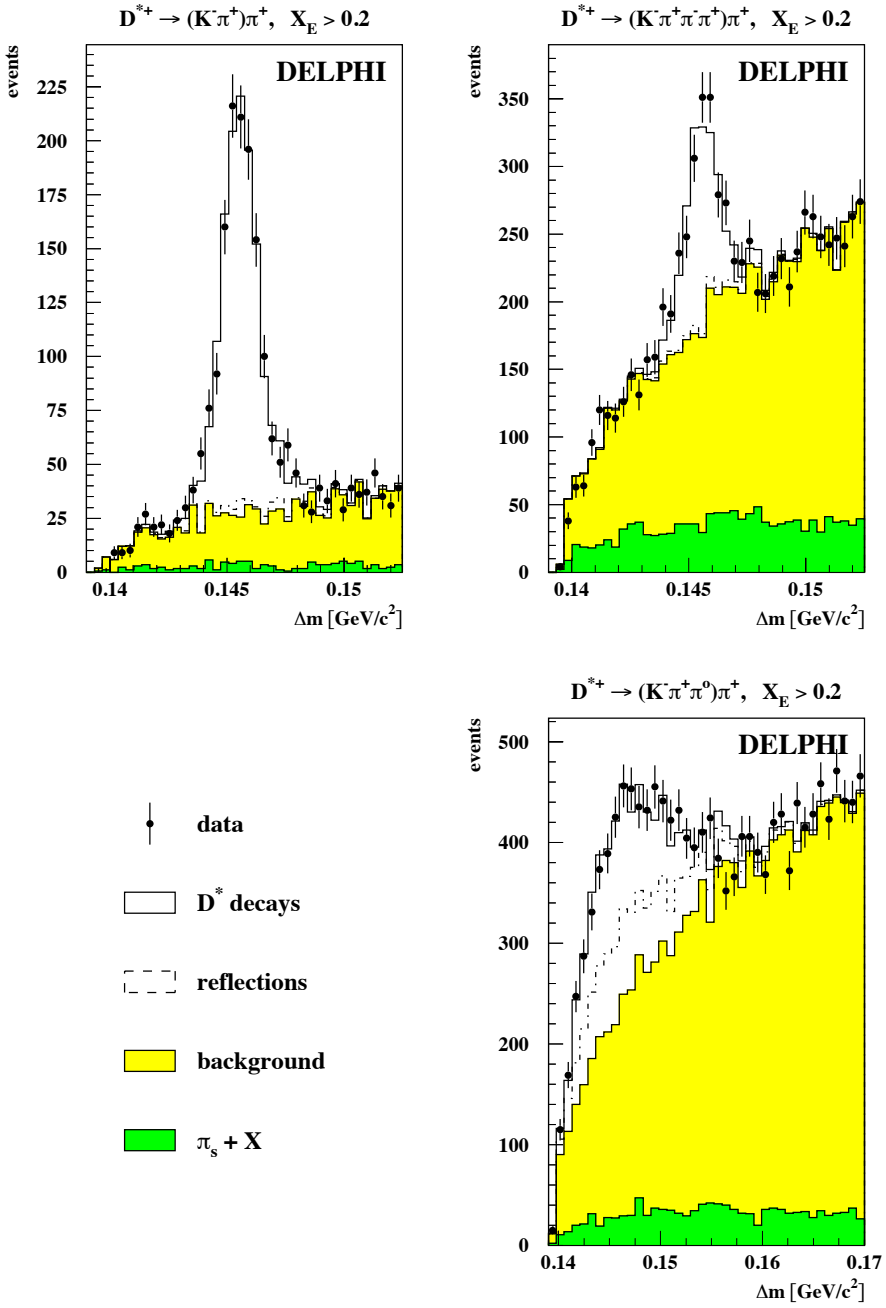

Figure 2: Mass spectra of the different D^* decay modes. The Monte Carlo contributions from reflections, partially reconstructed D^* decays and combinatorial background are also shown.

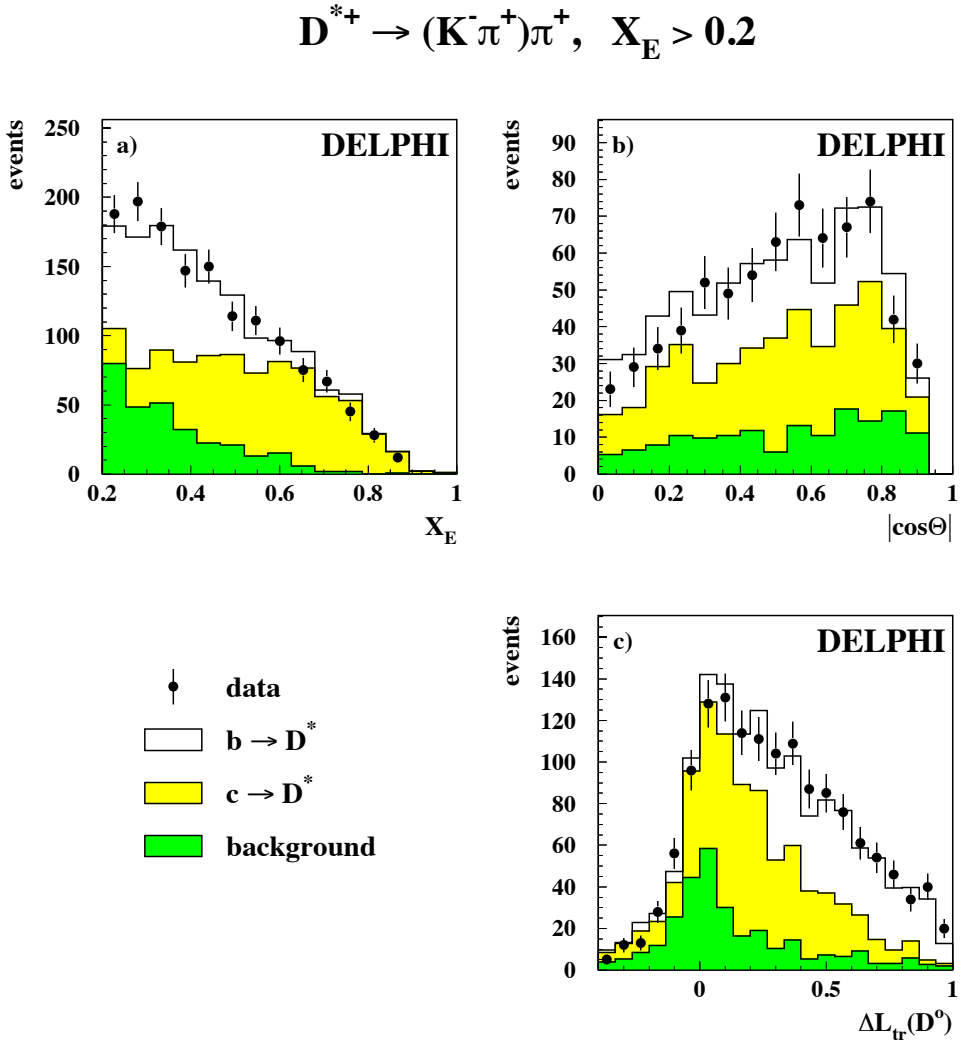

Figure 3: The scaled energy (a), polar angle (b) and transformed decay length (c) distribution of the different classes for the $D^{*+} \to (K^-\pi^+)\pi^+$ decay mode. The Monte Carlo is split into D^{*+} from charm and bottom events and combinatorial background. ($\Delta L_{tr} = \mathrm{sign}\Delta L \ (1 - e^{-2\Delta L})$)

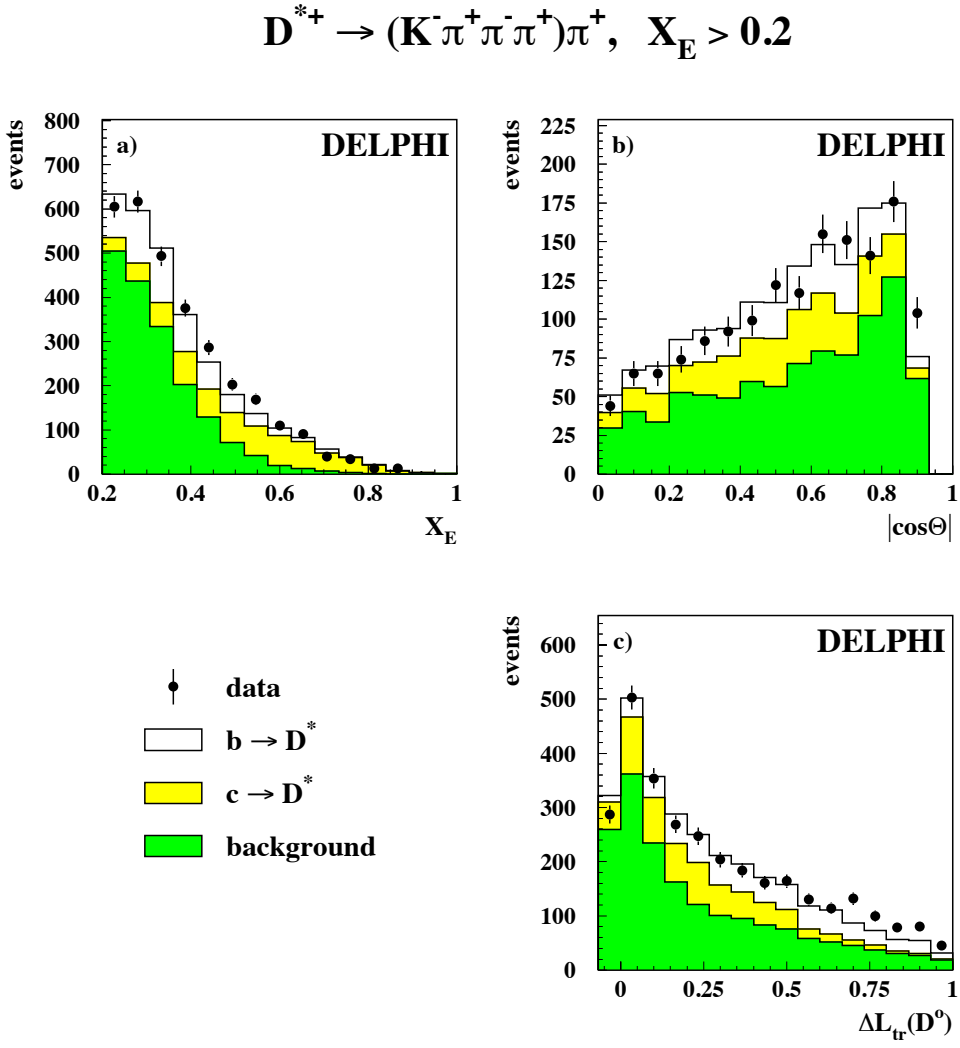

Figure 4: The scaled energy (a), polar angle (b) and transformed decay length (c) distribution of the different classes for the $D^{*+} \to (K^-\pi^+\pi^-\pi^+)\pi^+$ decay mode. The Monte Carlo is split into D^{*+} from charm and bottom events and combinatorial background. ($\Delta L_{tr} = \mathrm{sign}\Delta L \ (1 - e^{-2\Delta L})$)

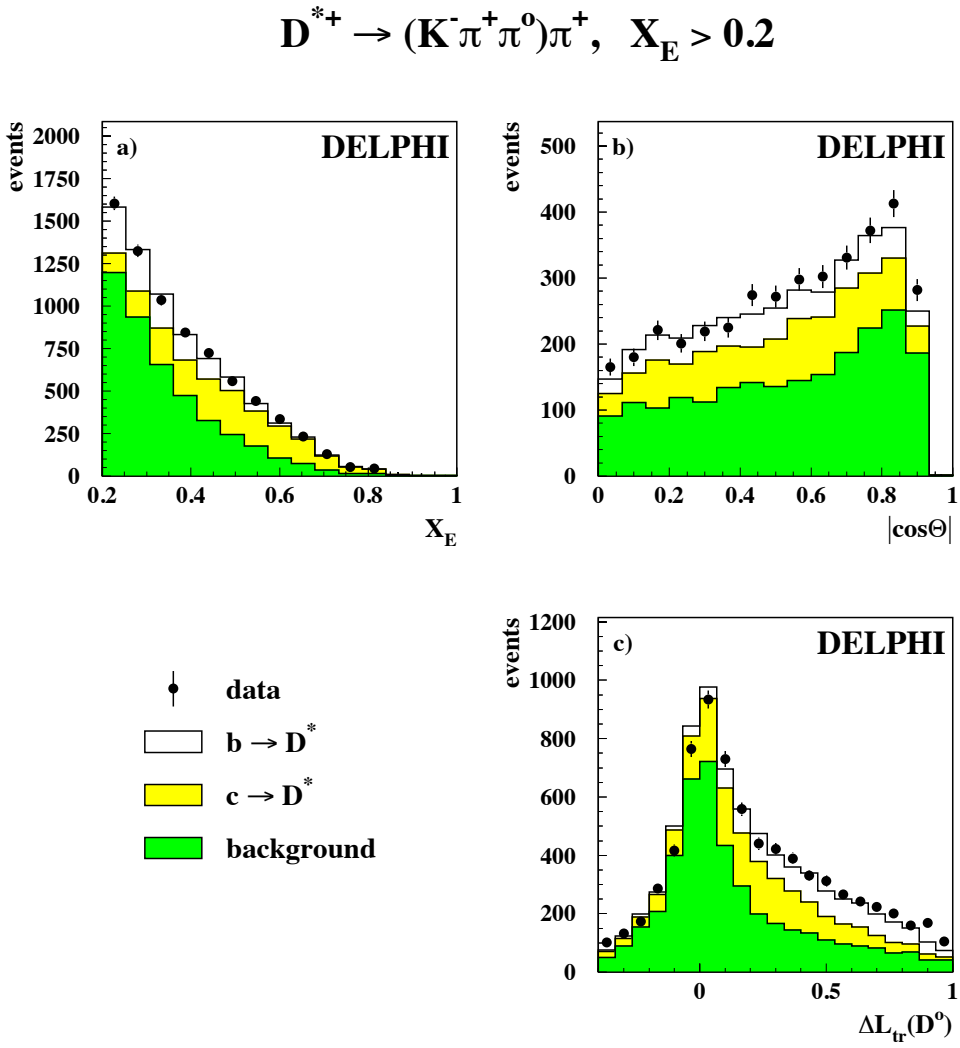

Figure 5: The scaled energy (a), polar angle (b) and transformed decay length (c) distribution of the different classes for the $D^{*+} \to (K^-\pi^+\pi^\circ)\pi^+$ decay mode. The Monte Carlo is split into D^{*+} from charm and bottom events and combinatorial background. ($\Delta L_{tr} = \mathrm{sign}\Delta L \ (1 - e^{-2\Delta L})$)

References

[1] M.Consoli et al., *Electroweak radiative corrections for Z physics*,
Z Physics at LEP Vol.1 p. 7-54, CERN 89-08, Geneva 1989

G.Burgers, F.Jegerlehner,
Δr, or the relation between the electroweak couplings and the weak vector boson masses,
Z Physics at LEP Vol.1 55-88, CERN 89-08, Geneva 1989

S.Jadach, W.Hollik, *Forward-backward asymmetries*,
Z Physics at LEP Vol.1 203-234, CERN 89-08, Geneva 1989

[2] H.-G. Moser, *B Mixing*, CERN PPE/93-164, Geneva 1993

[3] W. Venus, *b Weak Interaction Physics in High Energy Experiments*,
Proceedings of the Cornell Lepton Photon Conference, August 1993

[4] ALEPH Collaboration, D.Buskulic et al., Phys. Lett. B313 (1993) 498

[5] DELPHI Collaboration, *A Measurement of the B_d° oscillation frequency using the time evolution*,
DELPHI Note 93-81, Geneva 1993

[6] DELPHI Collaboration, P.Aarnio et al., Nucl. Inst. and Meth. A303 (1991) 233.

[7] DELPHI Collaboration, *DELSIM Reference Manual*, DELPHI Note 87-98, Geneva 1989

[8] P. Baillon, *Cherenkov ring search using a maximum likelihood technique*,
CERN/EP 84-171, Geneva 1984

[9] DELPHI Collaboration, P.Abreu et al., Z. Phys. C59 (1993) 533

[10] DELPHI Collaboration, P.Abreu et al., Phys. Lett. B276 (1992) 536

[11] T. Sjöstrand, *JETSET 7.3 Manual*, CERN TH/92-6488, Geneva 1992

[12] ALEPH Collaboration, D Buskuli et al., Z. Phy. C62 (1994) 1.

[13] OPAL Collaboration, R.Akers et al., Z. Phys. C60 (1993) 601

[14] Particle Data Group, Phys. Rev. D45 (1992) S1

[15] DELPHI Collaboration,
Measurement of the Forward Backward Asymmetry of $e^+e^- \to Z^0 \to b\bar{b}$ using prompt leptons and micro-vertex tag, DELPHI publication in preparation

[16] D.Bardin et al.,
ZFITTER: An Analytical Program for Fermion Pair Production in e^+e^- Annihilation,
CERN-TH. 6443/92, Geneva 1992

[17] CDF Collaboration, F.Abe et al,
Evidence for Top Quark Production in $p\bar{p}$ Collisions at sqrts $= 1.8$ TeV,
FERMILAB-PUB 94/097-E (1994)

[18] DELPHI Collaboration, P.Abreu et al., Z. Phys. C59 (1993) 21